Optimization of Thiazolidone Scaffolds Using Pocket Modeling for Development of Potential Secretory System Inhibitors of *Mycobacterium tuberculosis*

Mycobacterium tuberculosis'in Potansiyel Sekreter Sistem İnhibitörleri Olarak Thiazolidone İskelelerinin Optimizasyonu

🔘 Shivratna V. KHARE[1], 🔘 Sujata P. CHOUDHARI[2], 🔘 Siddharth P. PHALLE[1], 🔘 Santosh S. KUMBHAR[1], 🔘 Prafulla B. CHOUDHARI[1]*, 🔘 Sambhaji R. MASAL[1], 🔘 Aakash K. PATIL[1], 🔘 Rakesh P. DHAVALE[3], 🔘 Durgacharan A. BHAGWAT[3], 🔘 Atul M. KADAM[4]

[1]Bharati Vidyapeeth College of Pharmacy, Department of Pharmaceutical Chemistry, Computational Chemistry Research Lab, Kolhapur, India
[2]Sarojini College of Pharmacy, Department of Pharmaceutical Analysis, Kolhapur, India
[3]Bharati Vidyapeeth College of Pharmacy, Department of Pharmaceutics, Kolhapur, India
[4]Shree Santkrupa College of Pharmacy, Department of Pharmaceutics, Ghogaon, India

ABSTRACT

Objectives: *Mycobacterium tuberculosis* is the causative organism of tuberculosis, which is the most lethal disease after cancer in the current decade. The development of multidrug and broadly drug-resistant strains is making the problem of tuberculosis more and more critical. In the last 40 years, only one molecule has been added to the treatment regimen. Generally, drug design and development programs target proteins whose function is known to be essential to the bacterial cell. *M. tuberculosis* possesses specialized protein export systems like the SecA2 export pathway and ESX pathways.

Materials and Methods: In the present communication, rational development of an antimycobacterial agent's targeting protein export system was carried out by integrating pocket modeling and virtual analysis.

Results: The 23 identified potential lead compounds were synthesized, characterized by physicochemical and spectroscopic methods like infrared and nuclear magnetic resonance spectroscopy, and further screened for antimycobacterial activity using isoniazid as standard. All the designed compounds showed profound antimycobacterial activity.

Conclusion: We found that Q30, M9, M26, U8, and R26 molecules had significant desirable biological activity and specific interactions with Sec of mycobacteria. Further optimization of these leads is necessary for the development of potential antimycobacterial drug candidates with fewer side effects.

Key words: *Mycobacterium tuberculosis*, Sec, ESX, docking, antimycobacterial, multidrug resistant, pocket modeling

ÖZ

Amaç: *Mycobacterium tuberculosis*, son on yılda kanserden sonra en ölümcül hastalık olan tüberkülozun etkenidir. Çoklu ilaç ve ilaca dirençli suşların gelişimi, tüberküloz problemini daha da kritik kılmaktadır. Son 40 yılda, tedavi rejimine sadece bir molekül eklenmiştir. Genel olarak ilaç tasarım ve geliştirme programları, bakteri hücresi fonksiyonunda önemi olduğu bilinen proteinleri hedeflemektedir. *M. tuberculosis*, SecA2 ve ESX gibi özel protein ihracat sistemlerine sahiptir.

Gereç ve Yöntemler: Bu çalışmada, protein atım sistemini hedefleyen antimikobakteriyel bir bileşiğin rasyonel geliştirilmesi integre cep modelleme ve sanal analiz kullanılarak gerçekleştirilmiştir.

Bulgular: Yirmi üç bileşik tasarlanmış, sentezlenmiş, fizikokimyasal özellikleri ve infrared ve nükleer manyetik rezonans spektroskopisi ile yapıları karakterize edilmiştir. Ayrıca isoniazid standart olarak kullanılarak antimikobakteriyel etkileri saptanmıştır. Tasarlanan bileşiklerin hepsi iyi antimikobakteriyel aktivite göstermiştir.

Sonuç: Q30, M9, M26, U8 ve R26 moleküllerinin önemli biyolojik aktiviteye ve mikobakterilerin Sec ile spesifik etkileşime sahip olduğu bulunmuştur. Bu hedef bileşiklerin daha da iyileştirilmesi, daha az yan etkiye sahip potansiyel antimikobakteriyel ilaç adaylarının gelişimi için gereklidir.

Anahtar kelimeler: *Mycobacterium tuberculosis*, Sec, ESX, docking, antimikobakteriyel, çoklu ilaç direnci, cep modellemesi

INTRODUCTION

Tuberculosis is an air-borne disease caused by infection with *Mycobacterium tuberculosis.* In the current decade, tuberculosis has emerged as a global emergency due to its mortality rate.[1-3] Tuberculosis acts as the salient killer in patients suffering from immunocompromising diseases like acquired immune deficiency syndrome (AIDS) and diabetics. In more than 80% cases of AIDS death occurs in the patients due to tuberculosis.[4-7] The problem of multidrug resistant tuberculosis (MDR), extensively drug-resistant tuberculosis, and total drug-resistant tuberculosis has reached its peak.[8-11] Bedaquiline is the only newly developed and approved drug for active MDR tuberculosis in the last two decades. Negligence of pharmaceutical scientists and medicinal chemists towards tuberculosis generated this global problem of tuberculosis. A number of hurdles are normally associated with antitubercular drug discovery; one of them is *M. tuberculosis*. *M. tuberculosis* is lipid-rich gram-negative organism having specialized systems that make it different from other microorganisms.[12-15] Secretory systems are one of the specialized systems present in *M. tuberculosis*, and are key regulators of virulence of *M. tuberculosis*. In *M. tuberculosis* three different secretory systems, secondary translocase pathway (SEC), twin arginine translocation (TAT), and ESX, are present.[16-18] The SEC pathway is a major protein export system present in the mycobacterium, accounting for more than 50% of virulence protein exports in the mycobacterium. The SEC is a conserved protein pathway in the mycobacterium that does not have any homologues in the mammalian systems, and possesses ideal properties to act as a potential antimycobacterial drug target. The SEC pathway is a key enzyme involved in transport of the virulence protein across the cell membrane, which spreads tuberculosis all over the host body. Inhibition of SEC will be able to block the transport of the virulence protein, which will inhibit the spread of the tuberculosis. In recent years, a number of researchers have been trying to develop novel antitubercular agents targeting conserved protein targets. Currently a number of molecules like equisetin derivatives[19] and thiazolo[4,5-d] pyrimidine derivatives[20] are reported as SEC inhibitors. In this research article, an attempt was made to optimize thiazolidine scaffolds as potential SEC inhibitors via integration of pocket and pharmacophore modeling.

EXPERIMENTAL

Selection of target

M. tuberculosis has three specialized protein export systems: SEC, TAT, and ESX. The SEC is major protein export system of *M. tuberculosis*, exporting the bulk of virulent protein, which accounts for the spread of disease. SEC systems do not have any homologues in mammalian systems and so inhibition of this SEC will not lead to any toxicity to humans. Thus due to its critical role in the growth and virulence of the *M. tuberculosis*, the SEC has been selected as the preferred biomolecular target rather than TAT or ESX.

Pocket modeling of the selected protein export systems

Pocket modeling of the selected SEC of *M. tuberculosis* was carried out using the crystal structure of SEC downloaded from the free protein database www.rcsb.org. The downloaded crystal structure of SEC was first refined by the BioPredicta module, via removal of water molecules and retaining native hydrogen atoms in the protein structure. Pocket modeling of SEC A was carried out using the ProViz module of Vlife MDS 4.4. ProViz is an integrated property visualization module with which electrostatic and hydrophobic mapping of biomolecules can be carried out.

Design of molecules

Pocket modeling of the SEC revealed the binding pocket of SEC is U-shaped and highly hydrophobic, keeping in mind complementary structures on the thiazole template were designed with structural modification on the aromatic moiety carried out. A number of the aromatic benzaldehydes are utilized to generate a number of thiazole derivatives. Total 75×75 benzaldehyde combinations are utilized to generate total 5625 different structures (indicated as R) as shown in Table 1. These 5625 different thiazole derivatives were designed and drawn in 2D geometry using the builder module of Vlife MDS 4.4. 2D structures were converted into 3D geometry and their coordinates were optimized via energy minimization by application of Merck molecular force field.

Docking analysis of synthesized ligands

Molecular docking was performed to identify potent derivatives with the maximum binding affinity for SEC of *M. tuberculosis* amongst the designed set of molecules. Docking analysis was performed in the BioPredicta module of Vlife MDS 4.4 using grip-based docking analysis in which the protein structure was kept rigid and molecules were kept in flexible conformation so that a number of conformations can be achieved. The best 100 confirmations of all designed molecules were generated. Potent molecules were scrutinized based on binding energy and interaction profile. The proposed synthetic scheme of the designed derivatives is shown in Figure 1.

Screening based on the drug-like properties and percentage absorption

The designed set of molecules was analyzed for Lipinski parameters like molecular weight, H-bond acceptor, H-bond

Table 1. Designed set of molecules (total 75×75 benzaldehyde combinations are utilized to generate total 5625 different structures indicated as R)

| Sr. no.	R	Sr. no.	R	Sr. no.	R	Sr. no.	R
1.	C_6H_5	2.	$4-(CH_3)_2N-C_6H_5$	3.	$4CH_3CONH-C_6H_5$	4.	$2-OCHC_6H_5$
5.	$3-OCHC_6H_5$	6.	$4-OCHC_6H_5$	7.	$3-OCH,4-OCH_3-C_6H_4$	8.	$5-Br-2-OH-C_6H_4$
9.	$2-Br-C_6H_5$	10.	$3-Br-C_6H_5$	11.	$4-Br-C_6H_5$	12.	$2-Cl-6-F-C_6H_4$
13.	$4-Cl-3-NO_2$	14.	$2-Cl-C_6H_5$	15.	$3-Cl-C_6H_5$	16.	$4-Cl-C_6H_5$
17.	$2-(4-Cl-SC_6H_5)$	18.	$3-CN-C_6H_5$	19.	$4-CN-C_6H_5$	20.	$2,3-Cl-C_6H_4$
21.	$2,4-Cl-C_6H_4$	22.	$2,6-Cl-C_6H_4$	23.	$3,5-Cl-C_6H_4$	24.	$4-(C_2H_5)2N-C_6H_5$
25.	$2,6-F-C_6H_4$	26.	$3,4-F-C_6H_4$	27.	$2,3-OH-C_6H_4$	28.	$2,4-OH-C_6H_4$
29.	$2,5-OH-C_6H_4$	30.	$3,4-OH-C_6H_4$	31.	$2,3-OCH_3-C_6H_4$	32.	$2,4-OCH_3-C_6H_4$
33.	$2,5-OCH_3$	34.	$3,4-OCH_3-C_6H_4$	35.	$3,5-OCH_3-C_6H_4$	36.	$3,5-OCH_3,4-OH- C_6H_4$
37.	$2,4-CH_3-C_6H_4$	38.	$3,5-CH_3-C_6H_4$	39.	$3-OC_2H_5-4-OH-C_6H_4$	40.	$2-F-C_6H_5$
41.	$3-F-C_6H_5$	42.	$4-F-C_6H_5$	43.	$2-OH-C_6H_5$	44.	$3-OH-C_6H_5$
45.	$4-OH-C_6H_5$	46.	$2-OH,3-OCH_3-C_6H_4$	47.	$2-OH,4-OCH_3-C_6H_4$	48.	$2-OH,5-OCH_3-C_6H_4$
49.	$3-OH,4-OCH_3C_6H_4$	50.	$4-OH,3-OCH_3-5NO_2$	51.	$2-OH-5NO_2$	52.	$4-CH(CH_3)_2-C_6H_5$
53.	$2-OCH_3-C_6H_5$	54.	$3-OCH_3-C_6H_5$	55.	$4-OCH_3-C_6H_5$	56.	$4-CH_3-C_6H_5$
57.	$2-CH_3-C_6H_5$	58.	$3-CH_3-C_6H_5$	59.	$4-SCH_3-C_6H_5$	60.	$2-NO_2-C_6H_5$
61.	$3-NO_2-C_6H_5$	62.	$4-NO_2-C_6H_5$	63.	$3-OC_6H_5$	64.	$4-CH(CH_3)_3-C_6H_5$
65.	$2,3,5-Cl C_6H_3$	66.	$3,4,5-F-C_6H_3$	67.	$4-CF_3OCH_3-C_6H_4$	68.	$4-CF_3-C_6H_5$
69.	$2,3,4-OCH_3-C_6H_3$	70.	$3,4,5-OCH_3-C_6H_3$	71	$2,4,6-OCH_3-C_6H_3$	72.	$3-NO_2-C_6H_5$
73.	$C_5H_4O_2$	74.	$C_9H_{10}O_3$	75.	C_5H_4OS		
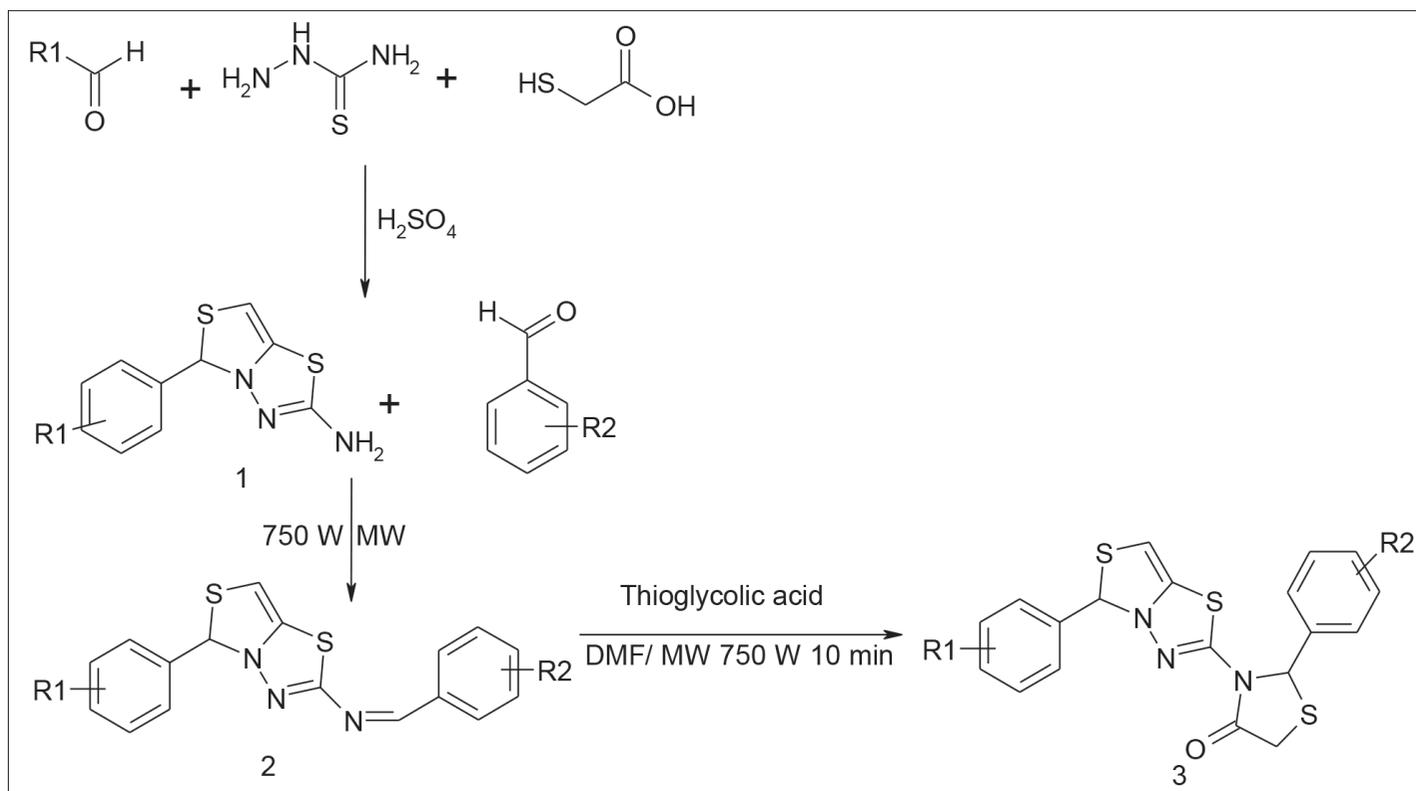
Figure 1. Synthetic scheme of designed derivatives

donor, rotatable bond, and XlogP. The physicochemical descriptors were calculated with the help of the QSAR module of Vlife MDS 4.4. Total polar surface area (TPSA) was calculated from the web server www.molinspiration.com/cgi-bin/properties by drawing the molecules in the drawing area and then calculating the TPSA. Percentage absorption was calculated using the formula;

% Absorption = 109 − (0.345 × TPSA).[21]

Synthesis of selected ligands[22]

Synthesis of optimized thiazole derivatives

Step 1

Synthesis of 2-amino-5-aryl-5H thiazolo[4,3-b]-l,3,4-thiadiazole (1)

To 25 mL of RBF were added aldehyde (0.02 M), thioglycolic acid (0.02 M), thiosemicarbazide (0.022 M), and 10 mL of concentrated H_2SO_4. The reaction mixture was mixed and left overnight and the resulting suspension was neutralized with 40% NaOH solution until the product was precipitated out and this resulting compound 1 was recrystallized from aqueous dioxane solution.

Synthesis of 1-phenyl-N-{5-phenyl-5H-[1,3]thiazolo[4,3-b][1,3,4]thiadiazol-2-yl}methanimine derivatives (2):

A solution of compound 1 (0.01 M) in ethanol (50 mL) was put in RBF and stirred vigorously for 15 min and to this resulting solution concentrated H_2SO_4 (2 mL) and aldehyde (0.01 M) were added. The reaction mixture was irradiated in a synthetic microwave (Cata 4R) for 10 min. The separated solid was filtered and recrystallized from ethanol.

Synthesis of 2-phenyl-3-{5-phenyl-5H-[1,3]thiazolo[4,3-b][1,3,4]thiadiazol-2-yl}-1,3- thiazolidin-4-one derivatives (3):

In 25 mL of RBF were added compound 2 (0.01 M) and thioglycolic acid (0.01 M) and then 30 mL of DMF was added followed by stirring. The resulting reaction mixture was irradiated in the microwave for 10 min at 750 W. The reaction mixture was cooled to room temperature and the resulting solid was separated and recrystallized from benzene to get compounds 1 to 23. Table 2 shows the list of substituents in the synthesized set of molecules.

B3: 3-[5-(4-bromophenyl)-5H-[1,3]thiazolo[4,3-b][1,3,4]thiadiazol-2-yl]-2-phenyl-1,3 thiazolidin-4-one

Color: Brown, Yield: 82%, m. p.: 192-194°C, MASS: [M+1] + 474.94, IR: 1752 cm⁻¹ (C=O Str.), 1452 cm⁻¹ (C=C), 2742.84 cm⁻¹ (Ar. CH), 1580 cm⁻¹ (-N=CH) NMR: ¹H NMR (DMSO-d_6, 300 MHz,): δ=6.95-7.35 (m, 9H, aromatic H), 4.95-5.90 (s, 2H, methine), 3.35 (s, 2H, methylene), 4.85 (s, 1H, ethylene).

C13: 2-(4-chlorophenyl)-3-{5-phenyl-5H-[1,3]thiazolo[4,3-b][1,3,4]thiadiazol-2-yl}-1,3-thiazolidin-4-one

Color: Yellow, Yield: 80%, m. p.: 178-180°C, MASS: [M+1] + 430.99, IR: 1690 cm⁻¹ (C=O Str.), 1435 cm⁻¹ (C=C), 2842 cm⁻¹ (Ar. CH), 1470 cm⁻¹ (-N=CH), NMR: ¹H NMR (DMSO-d_6, 300 MHz,): δ=6.90-7.25 (m, 9H, aromatic), 4.95-5.90 (s, 2H, methine), 3.38 (s, 2H, methylene), 4.95 (s, 1H, ethylene).

C1: 2-(2-chlorophenyl)-3-{5-phenyl-5H-[1,3]thiazolo[4,3-b][1,3,4]thiadiazol-2-yl}-1,3-thiazolidin-4-one

Color: Brown, Yield: 75%, m. p.: 186-188°C, MASS: [M+1] + 430.99, IR: 1625 cm⁻¹ (C=O Str.), 1400 cm⁻¹ (C=C), 2830 cm⁻¹ (Ar. CH), 1476 cm⁻¹ (-N=CH) NMR: ¹H NMR (DMSO-d_6, 300 MHz,): δ=6.95-7.20 (m, 9H, aromatic), 4.90-5.92 (s, 2H, methine), 3.30 (s, 2H, methylene), 4.90 (s, 1H, ethylene).

F1: 2-(2-chlorophenyl)-3-[5-(3,4-dimethoxyphenyl)-5H-[1,3]thiazolo[4,3-b][1,3,4]thiadiazol-2-yl]-1,3-thiazolidin-4-one

Color: Lemon, Yield: 89%, m. p.: 162-164°C, MASS: [M+1] + 492.02, IR: 1640 cm⁻¹ (C=O Str.), 1490 cm⁻¹ (C=C), 2790 cm⁻¹ (Ar. CH), 1520 cm⁻¹ (-N=CH) NMR: ¹H NMR (DMSO-d_6, 300 MHz,): δ=6.52-7.15 (m, 7H, aromatic), 4.95-5.90 (s, 2H, methine), 3.33 (s, 2H, methylene), 4.85 (s, 1H, ethylene), 3.75 (d, 6H, methyl).

O17: 2-(3-chlorophenyl)-3-[5-(2-hydroxyphenyl)-5H-[1,3]thiazolo[4,3-b][1,3,4]thiadiazol-2-yl]-1,3-thiazolidin-4-one

Color: Yellow, Yield: 80%, m. p.: 228-230°C, MASS: [M+1] + 447.97, IR: 1680 cm⁻¹ (C=O Str.), 1500 cm⁻¹ (C=C), 2810 cm⁻¹ (Ar. CH), 1580 cm⁻¹ (-N=CH) NMR: ¹H NMR (DMSO-d_6, 300 MHz,):

Table 2. List of substituents in synthesized set of molecules

Sr. no.	R1	R2	Code
1.	4-Br-C_6H_4	-C_6H_4	B3
2.	-C_6H_4	4-Cl-C_6H_4	C13
3.	-C_6H_4	2-Cl-C_6H_4	C1
4.	3,4-(OCH_3)-C_6H_4	2-Cl-C_6H_4	F1
5.	2-(OH)-C_6H_4	3-Cl-C_6H_4	O17
6.	-C_4H_3O	3-OCH_3-4-OH-C_6H_3	Q21
7.	4-$N(CH_3)_2$-C_6H_4	4-Cl-C_6H_4	L13
8.	2-(OH)-C_6H_4	4-Cl-C_6H_4	O13
9.	-C_4H_3O	2-(OH)-C_6H_4	Q24
10.	4-Cl-C_6H_4	4-(OH)-C_6H_4	M9
11.	4-F-C_6H_4	-C_4H_3O	H25
12.	3-Cl-C_6H_4	S-C_4H_3	R26
13.	3-(OCH_3)-4-(OH)-C_6H_3	-C_6H_4	V3
14.	3,5-$(OCH_3)_2$-4-(OH)C_6H_2	-C_6H_4	U8
15.	3-Cl-C_6H_4	3-NO_2-C_6H_4	A11
16.	2-Cl-C_6H_4	4-NO_2-C_6H_4	A10
17.	-C_4H_3O	3-OCH_3-C_6H_4	Q22
18.	-C_4H_3O	-$C_7H_5O_2$	Q30
19.	3-Cl-C_6H_4	S-C_4H_3	R25
20.	4-Cl-C_6H_4	S-C_4H_3	M26
21.	3-Cl-C_6H_4	3,4-$(OCH_3)_2$-C_6H_4	R6
22.	3-(OCH_3)-C_6H_4	4-Cl-C_6H_4	W13
23.	3-(OCH_3)-C_6H_4	4-F-C_6H_4	W8

δ=6.62-7.20 (m, 8H, aromatic), 4.95 (s, 1H, methine), 5.92 (s, 1H, methine), 3.38 (s, 1H, methylene), 4.75 (s, 1H, ethylene), 6.05 (s, 1H, aromatic C-OH).

Q21:   2-(3-ethoxy-4-hydroxyphenyl)-3-[5-(furan-2-yl)-5H-[1,3]thiazolo[4,3-b][1,3,4]thiadiazol-2-yl]-1,3-thiazolidin-4-one

Color: Black, Yield: 78%, m. p.: 192-194°C, MASS: [M+1] + 447.54, IR: 1750 cm⁻¹ (C=O Str.), 1540 cm⁻¹ (C=C), 2840 cm⁻¹ (Ar. CH), 1600 cm⁻¹ (-N=CH) NMR: ¹H NMR (DMSO-d_6, 300 MHz,): δ=6.05-7.30 (m, 6H, aromatic benzene and furan), 4.75 (s, 1H, ethylene), 5.15-5.92 (s, 2H, methine), 3.30 (s, 2H, methylene), 3.95 (s, 2H, methylene), 1.58 (s, 3H, methyl), 5.02 (s, 1H aromatic C-OH).

L13:   2-(4-chlorophenyl)-3-{5-[4-(dimethylamino)phenyl]-5H-[1,3]thiazolo[4,3-b][1,3,4]thiadiazol-2-yl}-1,3-thiazolidin-4-one

Color: Brown, Yield: 67%, m. p.: 156-158°C, MASS: [M+1] + 475.04, IR: 1652 cm⁻¹ (C=O Str.), 1538 cm⁻¹ (C=C), 2800 cm⁻¹ (Ar. CH), 1530 cm⁻¹ (-N=CH) NMR: ¹H NMR (DMSO-d_6, 300 MHz,): δ=6.45-7.20 (m, 8H, aromatic benzene), 4.80 (s, 1H, ethylene), 4.95-5.80 (s, 2H, methine), 3.30 (s, 2H, methylene), 2.95 (s, 6H, methyl N-CH₃).

O13:   2-(4-chlorophenyl)-3-[5-(2-hydroxyphenyl)-5H-[1,3]thiazolo[4,3-b][1,3,4]thiadiazol-2-yl]-1,3-thiazolidin-4-one

Color: Brown, Yield: 67%, m. p.: 236-238°C, MASS: [M+1] + 447.97, IR: 1760 cm⁻¹ (C=O Str.), 1540 cm⁻¹ (C=C), 2830 cm⁻¹ (Ar. CH), 1680 cm⁻¹ (-N=CH) NMR: ¹H NMR (DMSO-d_6, 300 MHz,): δ=6.65-7.25 (m, 8H, aromatic benzene), 4.85 (s, 1H, ethylene), 4.05-4.70 (s, 2H, methine), 3.28 (s, 2H, methylene), 5.25 (s, 1H, aromatic C-OH).

Q24:   3-[5-(furan-2-yl)-5H-[1,3]thiazolo[4,3-b][1,3,4]thiadiazol-2-yl]-2-(2-hydroxyphenyl)-1,3-thiazolidin-4-one

Color: Black, Yield: 75%, m. p.: 216-218°C, MASS: [M+1] + 403.49, IR: 1740 cm⁻¹ (C=O Str.), 1623 cm⁻¹ (C=C), 2810 cm⁻¹ (Ar. CH), 1680 cm⁻¹ (-N=CH), NMR: ¹H NMR (DMSO-d_6, 300 MHz,): δ=6.60-7.30 (m, 7H, aromatic benzene and furan), 4.80 (s, 1H, ethylene), 5.20-5.80 (s, 2H, methine), 3.30 (s, 2H, methylene), 5.25 (s, 1H, aromatic C-OH).

M9:   3-[5-(4-chlorophenyl)-5H-[1,3]thiazolo[4,3-b][1,3,4]thiadiazol-2-yl]-2-(4-hydroxyphenyl)-1,3-thiazolidin-4-one

Color: Brown, Yield: 88%, m. p.: 138-140°C, MASS: [M+1] + 447.97, IR: 1700 cm⁻¹ (C=O Str.), 1640 cm⁻¹ (C=C), 2790 cm⁻¹ (Ar. CH), 1650 cm⁻¹ (-N=CH) , NMR: ¹H NMR (DMSO-d_6, 300 MHz,): δ=6.55-7.25 (m, 8H, aromatic benzene), 4.85 (s, 1H, ethylene), 5.10-5.85 (s, 2H, methine), 3.38 (s, 2H, methylene), 6.05 (s, 1H, aromatic C-OH).

H25:   3-[5-(4-fluorophenyl)-5H-[1,3]thiazolo[4,3-b][1,3,4]thiadiazol-2-yl]-2-(furan-2-yl)-1,3-thiazolidin-4-one

Color: Yellow, Yield: 70%, m. p.: 122-124°C, MASS: [M+1] + 405.48, IR: 1688 cm⁻¹ (C=O Str.), 1589 cm⁻¹ (C=C), 2690 cm⁻¹ (Ar. CH), 1580 cm⁻¹ (-N=CH) NMR: ¹H NMR (DMSO-d_6, 300 MHz,): δ=6.30-7.05 (m, 7H, aromatic benzene and furan), 4.82 (s, 1H, ethylene), 5.10-5.85 (s, 2H, methine), 3.35 (s, 2H, methylene).

R26:   3-[5-(3-chlorophenyl)-5H-[1,3]thiazolo[4,3-b][1,3,4]thiadiazol-2-yl]-2-(thiophen-2-yl)-1,3-thiazolidin-4-one

Color: Yellow, Yield: 72%, m. p.: 206-208°C, MASS: [M+1] + 437.99, IR: 1750 cm⁻¹ (C=O Str.), 1670 cm⁻¹ (C=C), 2560 cm⁻¹ (Ar. CH), 1540 cm⁻¹ (-N=CH) NMR: ¹H NMR (DMSO-d_6, 300 MHz,): δ=6.60-7.10 (m, 7H, aromatic benzene and thiophene), 4.85 (s, 1H, ethylene), 4.95-5.90 (s, 2H, methine), 3.30 (s, 2H, methylene).

V3:   3-[5-(3-ethoxy-4-hydroxyphenyl)-5H-[1,3]thiazolo[4,3-b][1,3,4]thiadiazol-2-yl]-2-phenyl-1,3-thiazolidin-4-one

Color: Brown, Yield: 83%, m. p.: 180-182°C, MASS: [M+1] + 457.58, IR: 1620 cm⁻¹ (C=O Str.), 1560 cm⁻¹ (C=C), 2860 cm⁻¹ (Ar. CH), 1490 cm⁻¹ (-N=CH) NMR: ¹H NMR (DMSO-d_6, 300 MHz,): δ=6.45-7.14 (m, 8H, aromatic benzene), 4.80 (s, 1H, ethylene), 4.90-5.85 (s, 2H, methine), 3.35 (s, 2H, methylene), 5.95 (s, 1H, aromatic C-OH), 3.98 (s, 2H, methylene), 1.75 (s, 3H, methyl).

U8:   3-[5-(4-hydroxy-3,5-dimethoxyphenyl)-5H-[1,3]thiazolo[4,3-b][1,3,4]thiadiazol-2-yl]-2-phenyl-1,3-thiazolidin-4-one

Color: Yellow, Yield: 80%, m. p.: 230-232°C, MASS: [M+1] + 473.58, IR: 1688 cm⁻¹ (C=O Str.), 1562 cm⁻¹ (C=C), 2883 cm⁻¹ (Ar. CH), 1489 cm⁻¹ (-N=CH) NMR: ¹H NMR (DMSO-d_6, 300 MHz,): δ=5.95-7.10 (m, 7H, aromatic benzene), 4.85 (s, 1H, ethylene), 4.92-5.95 (s, 2H, methine), 3.28 (s, 2H, methylene), 5.98 (s, 1H, aromatic C-OH), 3.85 (s, 6H, methoxy).

A11:   3-[5-(3-chlorophenyl)-5H-[1,3]thiazolo[4,3-b][1,3,4]thiadiazol-2-yl]-2-(3-nitrophenyl)-1,3-thiazolidin-4-one

Color: Brown, Yield: 69%, m. p.: 146-148°C, MASS: [M+1] + 476.97, IR: 1679 cm⁻¹ (C=O Str.), 1575 cm⁻¹ (C=C), 2896 cm⁻¹ (Ar. CH), 1523 cm⁻¹ (-N=CH). NMR: ¹H NMR (DMSO-d_6, 300 MHz,): δ=6.90-7.95 (m, 8H, aromatic benzene), 4.75 (s, 1H, ethylene), 4.90-5.92 (s, 2H, methine), 3.33 (s, 2H, methylene).

A10:   3-[5-(2-chlorophenyl)-5H-[1,3]thiazolo[4,3-b][1,3,4]thiadiazol-2-yl]-2-(4-nitrophenyl)-1,3-thiazolidin-4-one

Color: Brown, Yield: 70%, m. p.: 174-176°C, MASS: [M+1] + 476.97, IR: 1590 cm⁻¹ (C=O Str.), 1456 cm⁻¹ (C=C), 2675 cm⁻¹ (Ar. CH), 1563 cm⁻¹ (-N=CH). NMR: ¹H NMR (DMSO-d_6, 300 MHz,): δ=7.04-8.05 (m, 8H, aromatic benzene), 4.85 (s, 1H, ethylene), 4.95-5.90 (s, 2H, methine), 3.28 (s, 2H, methylene).

Q22:   3-[5-(furan-2-yl)-5H-[1,3]thiazolo[4,3-b][1,3,4]thiadiazol-2-yl]-2-(3-methoxyphenyl)-1,3-thiazolidin-4-one

Color: Black, Yield: 78%, m. p.: 176-178°C, MASS: [M+1] + 417.52, IR: 1639 cm⁻¹ (C=O Str.), 1420 cm⁻¹ (C=C), 2640 cm⁻¹ (Ar. CH), 1570 cm⁻¹ (-N=CH). NMR: ¹H NMR (DMSO-d_6, 300 MHz,): δ=6.50-7.30 (m, 7H, aromatic benzene and furan), 4.80 (s, 1H, ethylene), 5.10-5.95 (s, 2H, methine), 3.30 (s, 2H, methylene), 3.75 (s, 3H, methoxy).

Q30:   2-(2H-1,3-benzodioxol-5-yl)-3-[5-(furan-2-yl)-5H-[1,3]thiazolo[4,3-b][1,3,4]thiadiazol-2-yl]-1,3-thiazolidin-4-one

Color: Black, Yield: 70%, m. p.: 240-242°C, MASS: [M+1] + 431.50, IR: 1782 cm^{-1} (C=O Str.), 1560 cm^{-1} (C=C), 2785 cm^{-1} (Ar. CH), 1630 cm^{-1} (-N=CH). NMR: ^{1}H NMR (DMSO-d_6, 300 MHz,): δ=6.45-7.25 (m, 6H, aromatic benzene and furan), 4.82 (s, 1H, ethylene), 5.15-5.85 (s, 2H, methine), 3.28 (s, 2H, methylene), 5.95 (s, 2H, 1,3-dioxole).

R25:   3-[5-(3-chlorophenyl)-5H-[1,3]thiazolo[4,3-b][1,3,4] thiadiazol-2-yl]-2-(thiophen-2-yl)-1,3-thiazolidin-4-one
Color: Yellow, Yield: 82%, m. p.: 234-236°C, MASS: [M+1] + 437.99 IR: 1700 cm^{-1} (C=O Str.), 1590 cm^{-1} (C=C), 2693 cm^{-1} (Ar. CH), 1578 cm^{-1} (-N=CH). NMR: ^{1}H NMR (DMSO-d_6, 300 MHz,): δ=6.65-7.05 (m, 7H, aromatic benzene and thiophene), 4.85 (s, 1H, ethylene), 4.95-5.95 (s, 2H, methine), 3.32 (s, 2H, methylene).

M26:   3-[5-(4-chlorophenyl)-5H-[1,3]thiazolo[4,3-b][1,3,4] thiadiazol-2-yl]-2-(thiophen-2-yl)-1,3-thiazolidin-4-one
Color: Brown, Yield: 70%, m. p.: 210-212°C, MASS: [M+1] + 437.99, IR: 1665 cm^{-1} (C=O Str.), 1545 cm^{-1} (C=C), 2530 cm^{-1} (Ar. CH), 1540 cm^{-1} (-N=CH). NMR: ^{1}H NMR (DMSO-d_6, 300 MHz,): δ=6.60-7.25 (m, 7H, aromatic benzene and thiophene), 4.82 (s, 1H, ethylene), 4.90-5.92 (s, 2H, methine), 3.35 (s, 2H, methylene).

R6:   3-[5-(3-chlorophenyl)-5H-[1,3]thiazolo[4,3-b][1,3,4] thiadiazol-2-yl]-2-(3,4dimethoxyphenyl)-1,3-thiazolidin-4-one
Color: Brown, Yield: 85%, m. p.: 226-228°C, MASS: [M+1] + 492.02, IR: 1675 cm^{-1} (C=O Str.), 1553 cm^{-1} (C=C), 2542 cm^{-1} (Ar. CH), 1580 cm^{-1} (-N=CH). NMR: ^{1}H NMR (DMSO-d_6, 300 MHz,): δ=6.50-7.15 (m, 7H, aromatic benzene), 4.82 (s, 1H, ethylene), 4.92-5.85 (s, 2H, methine), 3.33 (s, 2H, methylene), 3.75 (s, 6H, methoxy).

W13:   2-(4-chlorophenyl)-3-[5-(3-methoxyphenyl)-5H-[1,3] thiazolo[4,3-b][1,3,4]thiadiazol-2-yl]-1,3-thiazolidin-4-one
Color: White, Yield: 78%, m. p.: 170-172°C, MASS: [M+1] + 462.00, IR: 1600 cm^{-1} (C=O Str.), 1532 cm^{-1} (C=C), 2520 cm^{-1} (Ar. CH), 1560 cm^{-1} (-N=CH). NMR: ^{1}H NMR (DMSO-d_6, 300 MHz,): δ=6.55-7.20 (m, 8H, aromatic benzene), 4.85 (s, 1H, ethylene), 4.92-5.88 (s, 2H, methine), 3.30 (s, 2H, methylene), 3.78 (s, 3H, methoxy).

W8:   2-(4-fluorophenyl)-3-[5-(3-methoxyphenyl)-5H-[1,3] thiazolo[4,3-b][1,3,4]thiadiazol-2-yl]-1,3-thiazolidin-4-one
Color: Brown, Yield: 80%, m. p.: 160-162°C, MASS: [M+1] + 445.55 IR: 1750 cm^{-1} (C=O Str.), 1682 cm^{-1} (C=C), 2540 cm^{-1} (Ar. CH), 1670 cm^{-1} (-N=CH). NMR: ^{1}H NMR (DMSO-d_6, 300 MHz,): δ=6.65-7.05 (m, 8H, aromatic benzene), 4.80 (s, 1H, ethylene), 4.85-5.90 (s, 2H, methine), 3.34 (s, 2H, methylene), 3.65 (s, 3H, methoxy).

Antitubercular activity

The synthesized molecules were evaluated for antimycobacterial activity by culturing *Mycobacterium smegmatis* (NCIM 5138) on Middlebrook 7H9 broth (Difco) containing 0.5% albumin, 0.085% NaCl, 0.2% glucose, 0.05% Tween 80, and 0.5% glycerol at 37°C for 48 h to mid-log phase [optical density at 600 nm (OD$_{600}$)= 0.5]. Minimum inhibitory concentrations (MICs) of antibiotics against *M. smegmatis* were determined in Middlebrook 7H9 broth by the standard microdilution method. All synthesized derivatives were dissolved in dimethyl sulfoxide and utilized for the antimycobacterial assay in the concentration range of 3.25-1000 µg/mL.
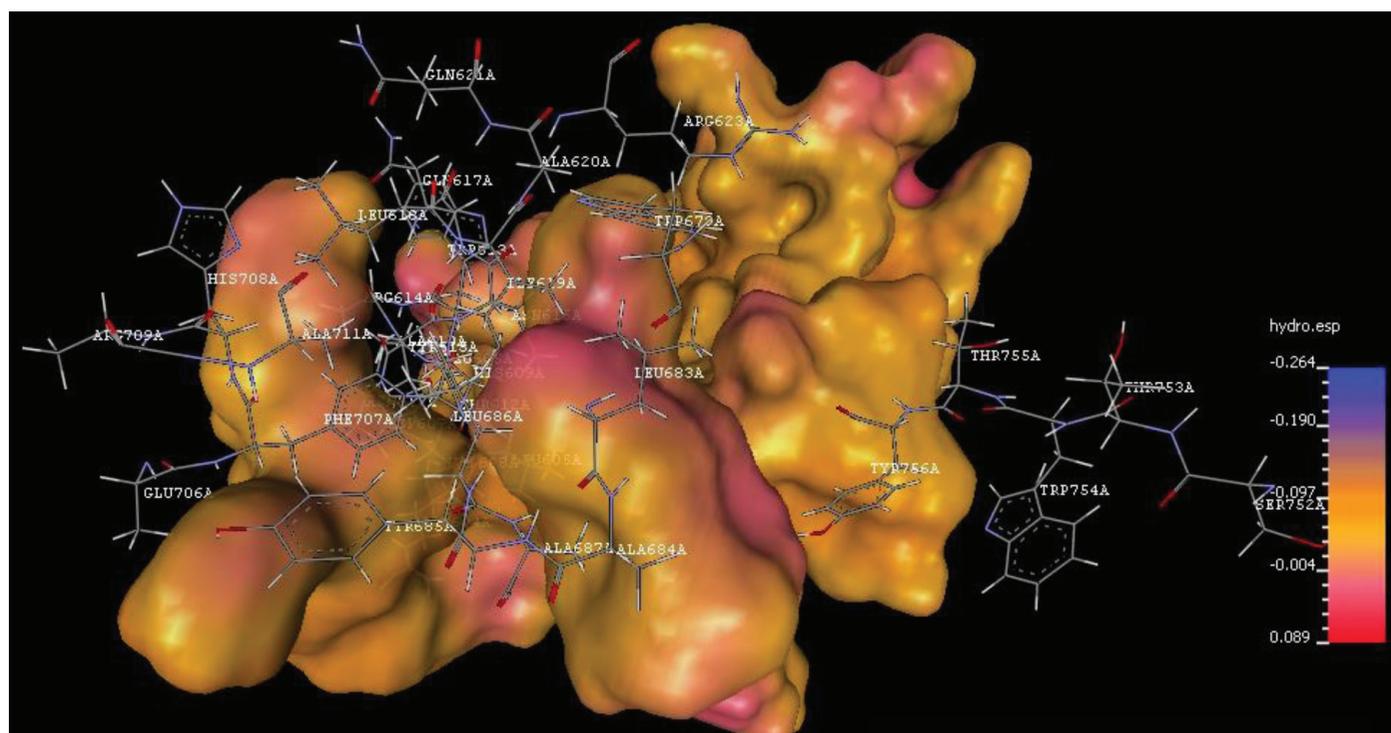

Figure 2. Hydrophobic map of active site of secondary translocase pathway of *Mycobacterium tuberculosis*

RESULTS AND DISCUSSION

Pocket modeling of SEC of M. tuberculosis

Binding pocket analysis was performed on the X-ray structure of the SEC from *M. tuberculosis* downloaded from free protein database www.rcsb.org. The ProViz module of Vlife MDS 4.4 was utilized to perform the pocket analysis. An electrostatic and hydrophobic map of the binding pocket of the SEC was generated to identify the relative orientation of critical amino acids. Pocket modeling of the SEC revealed its binding pocket is highly hydrophobic and ASP224, HIS534, and LYS115 are the three important amino acids required for ATP binding. Figure 2 shows the hydrophobic map of the active site of the SEC of *M. tuberculosis.* The SEC runs protein export, which is driven by ATP as the energy source, and inhibition of this ATP binding or blocking three amino acids will inhibit the SEC and ultimately protein export. The binding pocket of the SEC was found to be highly hydrophobic and U-shaped. Molecules were designed with the intent that they will retain necessary hydrophobicity and relative conformation with respect to the SEC of *M. tuberculosis*. Molecules were developed keeping thiazole as the template. Thiazole derivatives due the presence of two heteroatoms that will act as an anchor and two aromatic rings that will act as wings to the nucleus are capable of achieving the bioactive U- or V-shaped conformation, which is complementary to the binding site of the SEC. Aromatic benzaldehydes are utilized to manipulate the required hydrophobic characters from aromatic interaction with Histidine 534.

Screening based on the drug-like properties

Pharmacokinetic properties of the molecules are an important factor in the conversion of any New Chemical Entity to the drug. Pre-assessment of these drug-like properties plays a vital role in the selection of potential drug-like candidates from the designed data set of the molecules. All the molecules in the designed set of thiazole derivatives were assessed for Lipinski parameters like molecular weight, H-bond acceptor, H-bond donor, rotatable bond logp, and predicted oral absorption. In all,

Table 3. Table showing the molecules having the desired drug-like properties

Sr. no.	Compound code	Mole. wt.	H-acce	H-donor count	RBC	logP	TPSA (Å)	Pre. % oral abs.
1	A10	476.988	4	0	4	4.738	44.81	93.54
2	A11	476.988	4	0	4	4.738	81.4	80.91
3	B3	476.442	1	0	3	4.939	35.57	96.72
4	C1	431.99	1	0	3	4.83	35.57	96.72
5	C13	431.99	1	0	3	4.83	35.57	96.72
6	F1	492.043	3	0	7	4.847	54.04	90.35
7	H25	405.498	2	0	3	3.908	46.57	85.26
8	L13	475.059	2	0	6	4.896	41.37	94.72
9	M9	447.99	2	1	4	4.535	58.63	88.77
10	M26	438.019	1	0	3	4.891	35.57	96.72
11	O13	447.99	2	1	4	4.535	58.63	88.77
12	O17	447.99	2	1	4	4.535	58.63	88.77
13	Q21	447.56	3	1	7	3.873	81	81.05
14	Q22	417.534	2	0	5	3.778	57.95	89.00
15	Q24	433.533	3	1	6	3.483	81	81.05
16	Q30	431.517	1	0	3	3.498	67.18	85.82
17	R6	492.043	3	0	7	4.847	54.04	90.35
18	R25	421.952	1	0	3	4.423	48.71	92.19505
19	R26	438.019	1	0	3	4.891	35.57	96.72
20	U8	491.588	5	1	8	4.038	77.1	82.40
21	V3	457.598	3	1	7	4.28	67.86	85.58
22	W8	445.562	3	0	5	4.324	44.81	93.54
23	W13	462.017	2	0	5	4.838	44.81	93.54

TPSA: Total polar surface area, RBC: Red blood cell

Table 4. Binding interactions and energy of docked molecules

Sr. no.	Compound code	Binding energy	H-bond	Pi-stacking
1.	A10	-33.43	HIS534	HIS534
2.	A11	-0.12	HIS534	HIS534
3.	B3	-35.40	HIS534	HIS534
4.	C1	-7.41	ASP224	HIS534
5.	C13	-2.31	HIS534 HIS534	HIS534
6.	F1	-33.32	HIS534	HIS534
7.	L13	-8.74	HIS534	HIS534
8.	M9	-37.54	ASP219	HIS534
9.	M26	-38.54	ASP224	HIS534
10.	O13	-11.91	GLN498	HIS534
11.	O17	-9.81	HIS534	HIS534
12.	Q21	23.92	ASP219	HIS534
13.	Q22	-11.97	HIS534	HIS534
14.	Q24	-11.03	HIS534	HIS534
15.	Q30	-3.89	HIS534	HIS534
16.	R25	-2.51	HIS534	HIS534
17.	R26	-4.66	ASP224	HIS534
18.	R6	-11.74	HIS534	HIS534
19.	U8	-0.21	HIS534	HIS534
20.	V3	-36.40	HIS534	HIS534
21.	H25	-8.37	HIS534	HIS534
22.	W8	-33.40	ASP224	HIS534
23.	W13	-31.56	HIS534	HIS534

Figure 4. Showing the posed molecule U8 (Ball and Stick) with PDB ID 4UAQ with hydrogen bond interaction (red color)

23 derivatives were found to have the desired pharmacokinetic properties and predicted oral absorption <70%. The selected 23 derivatives with the drug-like properties are given in Table 3.

Molecular docking

Molecular docking was utilized to predict the potential active inhibitors from the designed set of ligands. Grip-based docking analysis was performed maintaining the SEC in rigid conformation and ligands in flexible conformation. All the design set of molecules were found to be binding to the same binding site to that of ATP in the SEC. The designed set of molecules was found to be interacting with HIS 534 and ASP224 via formation with hydrogen bond interaction and pi-stacking interaction. Binding interactions of the 23 selected molecules are summarized in Table 4, while Figures 3, 4, 5, and 6 show the most active conformation of molecules M26, U8, R26, and A10 (Ball and Stick) with PDB ID 4UAQ, respectively.

Biological activity

The antimycobacterial activity of the synthesized derivatives was determined against the standard *M. smegmatis* (NCIM No: 5138). *M. smegmatis* is an organism belonging to the family Mycobacterium having nearly 80% genome similarity with *M. tuberculosis.* Isoniazid was utilized as the positive standard for the antimycobacterial activity. MICs of all 23 derivatives are summarized in Figure 7. All the compounds showed good to moderate activity against the tested strain. Compounds R26, Q30, and M9 showed maximum antitubercular activity (MIC: 62.5 µg/mL). The excellent activity of M9 and R26 indicates halogens have a positive effect on antitubercular activity, and the activity of Q30 is an interesting finding that indicates substitution of the heterocyclic nucleus will also potentiate the activity. Derivative L13 showed good activity (MIC: 125 µg/mL), which justifies the substitution of halogen in the aromatic ring. A10, C13, F1, O13, O17, Q21, Q22, Q24, R25, R6, U8, and W13 are moderately active compounds with MIC: 500 µg/mL.

Figure 3. Figure showing posed molecule M26 (Ball and Stick) with PDB ID 4UAQ with hydrogen bond interaction (red color) and Pi-Stacking Interaction (blue colour)
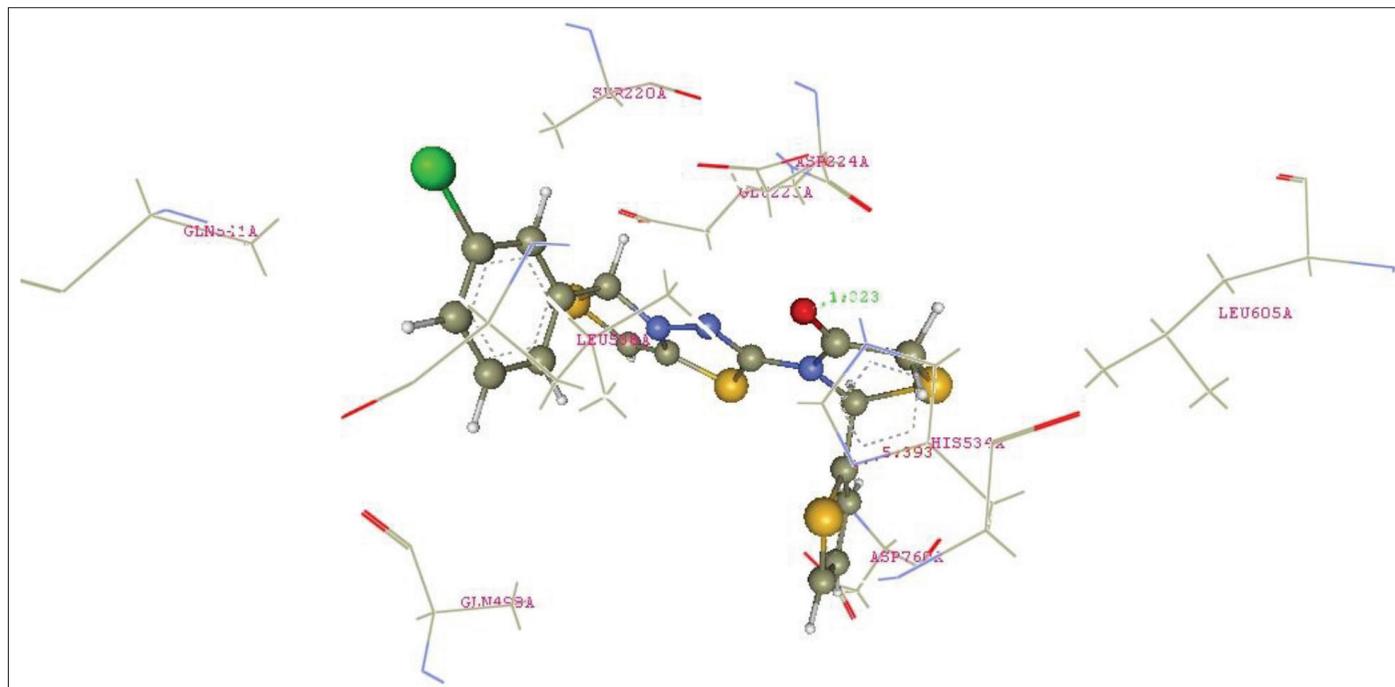
Figure 5. Showing the posed molecule R26 (Ball and Stick) with PDB ID 4UAQ with hydrogen bond interaction (red color)
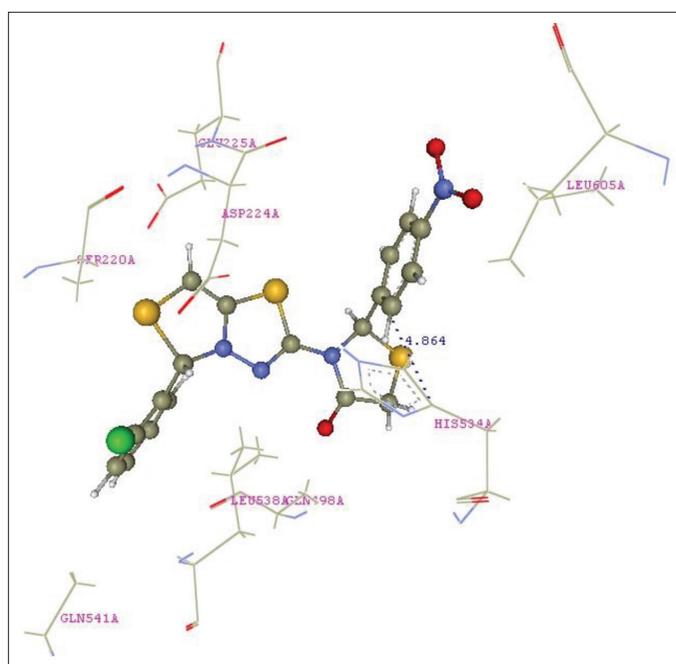

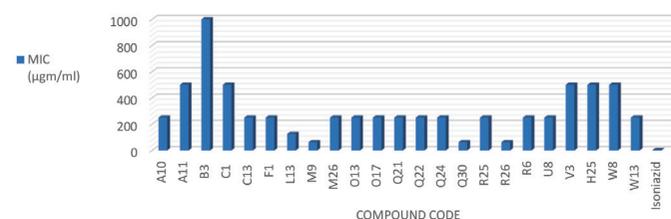**Figure 6.** Showing the posed molecule A10 (Ball and Stick) with PDB ID 4UAQ

Figure 7. Designed compounds with minimum inhibitory concentration

CONCLUSIONS

Attempts to design and develop molecules targeting secretory systems of *M. tuberculosis* yielded the following significant findings. Identification and validation of secretory systems as targets for antitubercular drug design and discovery were successfully carried out. Out of the three protein export systems associated with *M. tuberculosis* the SEC protein export system was utilized successfully for the development of antitubercular agents that are selective and can be utilized against all resistant forms of tuberculosis. Protein export systems are conserved systems and they have no isoform in humans and so targeting protein export systems will be the potential route for the development of selective and active antitubercular agents. Pocket modeling of the active site or binding site of the SEC revealed an interesting fact about the size and shape of the binding pocket of the SEC and signified the development of hydrophobic ligands for binding with the SEC of *M. tuberculosis*. Based on the pocket modeling data and literature survey in total 5184 molecules were designed around the thiazole scaffold via the change in the different aromatic benzaldehyde structures. Moreover, 5625 designed molecules were further scrutinized via Lipinski drug-like properties and toxicity profile using OCHEM and for binding efficiency using molecular docking analysis. The results of all three analyses yielded 23 potent, selective molecules successfully synthesized via reaction of an aromatic aldehyde, thiosemicarbazide, and thioglycolic acid. All the molecules were successfully synthesized using microwave-assisted synthesis, which improved the yield and reduced the time of reaction compared to the procedures reported in the literature. All 23 derivatives synthesized were characterized via all physicochemical methods, melting point, and IR and NMR spectroscopy. Halogen-substituted derivatives

showed significant activity, which indicates substitution of an electron-withdrawing group in the aryl ring will potentiate antimycobacterial activity. M26, U8, and R26 molecules have significant desirable biological activity and specific interactions with the SEC. Further optimization of these leads is necessary for the development of potential antitubercular drug-like candidates. These potential drug candidates with specific SEC inhibitory properties resulted from the utilization of integration of pocket modeling and virtual screening.

Conflict of Interest: No conflict of interest was declared by the authors.

REFERENCES

1. Abagyan R, Totrov M, High-throughput Docking for Lead Generation. Curr Opin Chem Biol. 2001;5:375-382.

2. Alam S, Khan F. QSAR and Docking studies on Xanthone Derivatives for Anticancer Activity Targeting DNA topoisomerase IIα. Drug Des Devel Ther. 2014;8:183-195.

3. Bermudez LE, Goodman J. *Mycobacterium tuberculosis* invades and replicates within Type II alveolar cells. Infect Immun. 1996;64: 1400-1406.

4. Bhatia MS, Ingale KB, Choudhari PB, Bhatia NM, Sawant RL. Application quantum and physicochemical molecular descriptors utilizing principal components to study the mode of anticoagulant activity of pyridyl chromen-2-one derivatives. Bioorg Med Chem. 2009;17:1654-1662.

5. Borrell S, Gagneux S. Infectiousness, reproductive fitness, and evolution of drug-resistant *Mycobacterium tuberculosis*. Int J Tuberc Lung Dis. 2009;13:1456-1466.

6. Brodin P, Majlessi L, Marsollier L, de Jonge MI, Bottai D, Demangel C, Hinds J, Neyrolles O, Butcher PD, Leclerc C, Cole ST, Brosch R. Dissection of ESAT-6 system of *Mycobacterium tuberculosis* and impact on immunogenicity and virulence. Infect Immun. 2006;74:88-98.

7. Choudhari PB, Bhatia MS, Bhatia NM. Application of Pocket Modeling and k-nearest Neighbor Molecular Field Analysis (kNN-MFA) for Designing of some Anticoagulants: Potential Factor IXa Inhibitors. Medicinal Chemistry Research. 2012;19:3-5.

8. Choure R, Pitre KS. Structural modification of coumarin for its increased anticoagulation potency. Canadian J Chem Engineering Technology. 2010;1:7-15.

9. Derrick SC, Morris SL. The ESAT6 protein of *Mycobacterium tuberculosis* induces apoptosis of macrophages by activating caspase expression. Cell Microbiol. 2007;9:1547-1555.

10. Ducati RG, Ruffino-Netto A, Basso LA, Santos DS. The Resumption of Consumption - A Review on Tuberculosis. Mem Inst Oswaldo Cruz. 2006;101:697-714.

11. Feltcher ME, Sullivan JT, Braunstein M. Protein Export Systems of *Mycobacterium tuberculosis*: novel target for drug development. Future Microbiol. 2010;5:1581-1597.

12. Fenton MJ, Vermeulen MW. Immunopathology of tuberculosis: roles of macrophages and monocytes. Infect Immun. 1996;64:683-690.

13. Finlay BB, Falkow S. Common themes in microbial pathogenicity revisited. Microbiol Mol Biol Rev. 1997;61:136-169.

14. Fortune SM, Jaeger A, Sarracino DA, Chase MR, Sassetti CM, Sherman DR, Bloom BR, Rubin EJ. Mutually dependent secretion of proteins required for mycobacterial virulence. Proc Natl Acad Sci USA. 2005;102:10676-10681.

15. Ginsberg AM. Tuberculosis drug development: Progress challenges and the road ahead. Tuberculosis (Edinb). 2010;90:162-167.

16. Jain A, Mondal R. Extensively drug-resistant tuberculosis: current challenges and threats. FEMS Immunol Med Microbiol. 2008;53:145-150.

17. Keane J, Balcewicz-Sablinska MK, Remold HG, Chupp GL, Meek BB, Fenton MJ, Kornfeld H. Infection by *Mycobacterium tuberculosis* promotes human alveolar macrophages apoptosis. Infect Immun. 1997;65:298-304.

18. Leung AN. Pulmonary Tuberculosis: The Essentials. Radiology. 1999;210:307-322.

19. Sugie Y, Inagaki S, Kato Y, Nishida H, Pang CH, Saito T, Sakemi S, Dib-Hajj F, Mueller JP, Sutcliffe J, Kojima Y. CJ-21,058, a new SecA inhibitor isolated from a fungus. J Antibiot (Tokyo). 2002;55:25-29.

20. Jang MY, De Jonghe S, Segers K, Anné J, Herdewijn P. Synthesis of novel 5-amino-thiazolo[4,5-d]pyrimidines as *E. coli* and *S. aureus* SecA inhibitors. Bioorg Med Chem. 2011;19:702-714.

21. Tripathi L, Kumar P, Singh R, Stables JP. Design, synthesis and anticonvulsant evaluation of novel N-(4-substituted phenyl)-2-[4-(substituted) benzylidene]-hydrazinecarbothioamides. Eur J Med Chem. 2012;47:153-166.

22. Malipeddi H, Karigar AA, Malipeddi VR, Sikarwar MS. Synthesis and Antitubercular Activity of Some Novel Thiazolidinone Derivatives. TroJ of Pharm Res. 2012;11:611-620.